Mechanical behaviour of repair mortars

Abdenour Alliche, Amjad Mallat

Mechanical behaviour of repair mortars.

Abdenour Alliche[1*], Amjad Mallat[2]

[1]*UPMC Univ. Paris 6, UMR 7190, Institut Jean Le Rond d'Alembert, F-75005 Paris France*
*abdenour.alliche@upmc.fr
[2]*CNRS Liban, P.O. Box 11-8281, Ryad El Solh 11 07 2260, 59 Zahia Selman Street, Beirut, Lebanon*

ABSTRACT. We investigate two repair mortars using mechanical tests specifically developed for this type of material. The first one is a fiber reinforced lime-based mortar, which contains thickening agent and limestone additions. The second one is a fiber reinforced ordinary mortar, which contains a small quantity of silica fume and additives. The mechanical characterization of the materials is based on tension, compression, and three-point bending tests. The bond between the repair mortars and substrate was investigated by slant shear and flexural bonding tests. The results obtained have demonstrated the influence of the surface roughness and moisture conditions on the bond strength. Finally, Scanning Electron Microscopic observations have showed the morphology of the repair mortar-to-substrate interfacial zone.

RÉSUME. Deux mortiers de réparation ont été étudiés à l'aide d'essais mécaniques spécifiquement développés pour ce type de matériaux. Le premier mortier est à base de chaux contenant des fibres organiques, des agents épaississants et des additions de calcaire. Le second est un mortier ordinaire contenant également des fibres organiques, de la fumée de silice et d'autres additifs. La caractérisation mécanique a été réalisée à l'aide des essais de traction, de compression et de flexion trois points. L'adhérence entre les mortiers de réparation et le substrat a été étudiée en utilisant des tests de cisaillement oblique et des tests de flexion. Les résultats obtenus ont démontré l'influence de la rugosité de surface et les conditions d'humidité sur la résistance du collage. Enfin, des observations au microscope électronique à balayage ont montré la morphologie de la zone interfaciale entre le mortier de réparation et le substrat.

KEYWORDS: Repair mortars, Mechanical behaviour, Interfacial zone, Bond strength.

MOTS CLÉS : Mortiers de réparation, comportement mécanique, interface, adhérence.

1. Introduction

Many buildings and structures were constructed using concrete and reinforced concrete during the last century. These materials are subjected to mechanical and chemical aggressive environment. Their rehabilitation generates financial costs. Repair refurbishment and maintenance of concrete structures have become a significant part of the total cost of construction worldwide (Mangat *et al.* 1997).

Different repair methods and materials are currently used to overcome damage in deteriorated structures. The mechanical properties and physicochemical damaged substrates determine the type of repair material and the technique used (Wall *et al*. 1998, Tabor *et al.* 1978). Repair mortars based on cement and organic fibers are the most commonly used materials. In the hardened mortar, fibers prevent the microcracks from developing into macrocracks (Pascal *et al.* 2004). The property enhancement of fiber-reinforced mortar can be largely attributed to the crack bridging forces provided by the fibers which limit crack opening and distribute the stresses to the nearby matrix, thus suppressing strain localization. Consequently, the strength and strain capacity of the composite are increased appreciably (Chorinsky 1986, Li *et al.* 2001).

Design is usually based on the experience of specialist contractors and when the selection of repair materials is made, emphasis is normally given to their relative short-term properties such as strength and bond and early age plastic shrinkage/expansion. Although these properties indicate the immediate performance of the repair. Therefore, there is an important need for recognizing and understanding the properties evolution of repair materials, which are of significance to the subsequent structural behaviours of repaired concrete members. An important factor for the success of repair works in concrete structures is to realize sufficient bonding between the repair material and the substrate (Li *et al.*. 2001, Jolio *et al*. 2004, Emmons 1994).

The study presents an experimental method to investigate the mechanical behaviour and bonding capacity of two fiber-reinforced repair mortars. For this purpose, a range of surface roughness with various substrate moisture conditions was studied by slant-shear and flexural bonding tests.

We describe in section 2 the different mortars studied and the samples preparation. A summarize of characteristics of these mortars in terms of shrinkage, porosity, cement hydration, and other material properties is also given in this section. Section 3 gives a description of the shrinkage, compression, three-point bending and tensile tests. The results obtained are presented in Section 4, followed by a discussion of the behaviour observed. Bond characterization between substrate and repair mortars is presented and discussed.

2. Materials and sample preparation

Two repair mortars reinforced with short fibers have been selected and studied. The mortars are ready for on-site mixing and use and require only the addition of water. The fibers have circular cross sections with diameter of 25 μm and two lengths according to the repair mortar. The porosity of the 28-days old mortars was obtained by mercury intrusion porosimetry. Details of these repair materials are presented briefly below:

FLM is a fiber reinforced lime-based mortar. It consists of sand, limestone, special hydraulic binder, lime, polyacrylonitryle fibers, thickening agent and additives. The fibers length and percentage in the composites was 4 mm and 0.3% weight respectively. FLM resists sea and sulfated water. A water-dry powder mixture ratio of 0.212 is recommended.

FOM is a non-shrinkable fiber reinforced ordinary mortar. It consists of sand, ordinary cement, polyacrylonitryle fibers, small quantity of silica fume and additives. The fibers length and percentage in the composites was 8 mm and 0.2% weight respectively. FOM resists carbonation, sea and sulfated water. A water-dry powder mixture ratio of 0.14 is recommended.

OM is ordinary mortar prepared using CEMII 32.5R cement. The mix proportions (by weight) were 1 : 3.68 : 0.48 (cement : sand : water), to achieve 28 days compressive strength of 25 MPa and of 20 GPa Young's modulus.

Physical and mechanical properties of the two mortars are presented in Table 1.

All samples were molded and cured for 24 hours in the atmosphere of the laboratory. After demolding, samples were stored in a relatively dry atmosphere 50% RH and 23°C for 28 days. All mortars were mixed in a conventional blade-type concrete mixer.

Tensile tests were carried out on samples with cylindrical central gauge zone (40 mm diameter, 30 mm height). Specimens were designed and manufactured so as to circumscribe damage and localization of crack in a zone named gage zone (figure 2). The materials were cast in three layers in a silicone cylindrical mold of 40 mm diameter on a vibrating table (50 Hz, 10 s/layer).

Compression test samples were cast in (40 mm diameter and 80 mm height) cylindrical mold.

Flexural samples were cast in (40x40x160 mm^3) prismatic mold.

The slant-shear test substrates were cast in (40 mm diameter and 80 mm height) half-cylindrical mold with the interface line at 30 °C to the vertical. Surfaces are treated to obtain various roughnesses. Four surface preparation methods were used to obtain smooth grounded, hand-engraved, steel-brushed/sand-blasted and as broken surfaces. After the preparation of the surfaces, the substrates were stored under four moisture conditions to obtain dry substrate with dry surface, wet substrate with dry surface, saturated substrate with dry surface and saturated substrate with saturated surface. Only wet substrates with dry surfaces were used for flexural bonding tests. The loaded faces of the compression and slant-shear

compression test samples were covered by thin layers of sulfur to be parallel and flat.

Sample	Grain size (mm)	Fiber content (by weight)	Fiber length (mm)	Fiber diameter (mm)	Open porosity	Density Mortar
FOM	0 -2	0.3%	8	0.25	23%	2.08
FLM	0 – 1.25	0.2%	4	0.25	31%	1.82
OM	0 – 0.8	no fiber	no fiber	no fiber	24%	2

Table 1. *Physical characteristics of mortars*

3 Experimental tests

3.1. *Shrinkage strain measurement*

Shrinkage of the repair mortar at early age is a major cause of cracking. This phenomenon results from residual stress in the weak mortar. Shrinkage strain measurements were carried out on 40x40x160mm^3 mortar samples. The displacement of the upper sample face was measured by mechanical dial gauge with radial retractable stem (figure 1.).

Figure 1. *Experimental setup for shrinkage strain measurement*

3.2. *Three-point bending tests*

A sketch of the experimental setup is given in figure 2. The three-point bending tests were performed on the 40x40x160 mm^3 samples, using an INSTRON 4505

type machine equipped with a 5 kN load cell and a PID servo control. A strain measurement was achieved on the face under tensile stress using an INSTRON extensometer. The PID servo control allowed us to rule the tests under strain control conditions. The tests were carried out on mortars at various ages between 7 and 210 days. At least five samples were tested for each age. Figure 2 shows a typical load versus tensile strain diagram. The ascending part of the curve is quasi-linear. However, near the top of the curve, the slope exhibits a slight decrease which indicates the damage initiation. At peak load, the micro-cracks coalesce into an unstable crack. The decreasing part of the curve corresponds to the propagation of this crack, which induces a loss of sample stiffness.

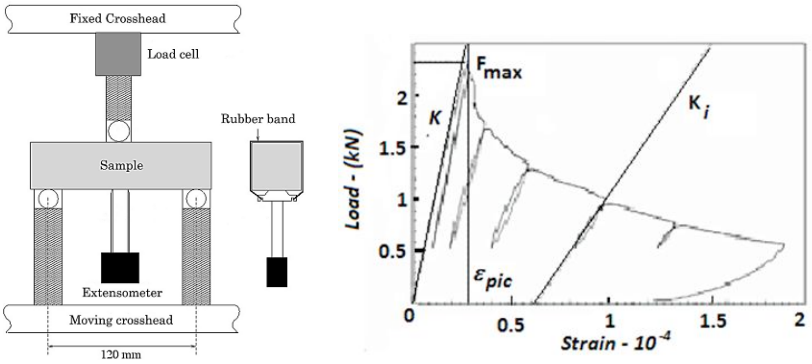

Figure 2. *Experimental setup for three-point bending test and typical load strain curve.*

3.3. *Tensile tests*

Tensile tests allow a direct measurement of material properties. This test is however quite difficult to implement in the case of brittle materials such concretes and mortars (Ramtani *et al.* 1990). We performed two tests called direct and modified tensile test. The principle of the modified tensile test is to stabilize cracks in the material by inserting metallic bar in the mortar sample. This allows reaching post peak stage of the stress strain diagram.

3.3.1. Direct tensile test

Direct tensile test presented in figure 4 (a) includes loading fixture with a ball joint for avoiding possible bending effects in the specimen. Mortar strain measurement is recorded by two INSTRON extensometers with a working range of 2.5 mm and gauge length of 25 mm, mounted on the opposite sides of the gage zone.

All Direct tensile tests were achieved under displacement control. The displacement rate was set to: 3.10^{-3} mm.s^{-1}.

Figure 3 shows stress-strain curves of FOM, FLM and ordinary mortar obtained under direct tensile test. The mortars show a linear behaviour until unstable failure. These tests allow studying the elastic behaviour of the materials; however none of these tests allow reaching the post-peak behaviour of the materials.

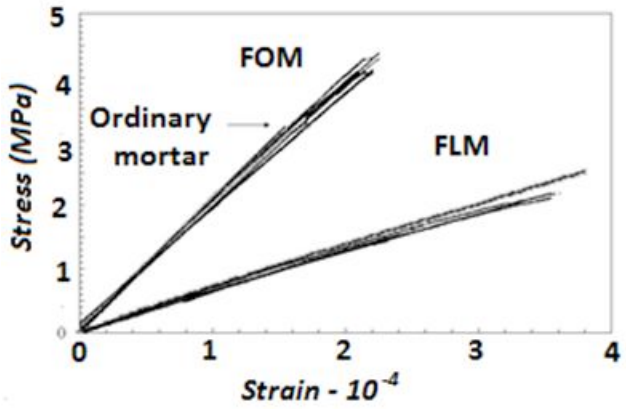

Figure 3. *Tensile curves of the mortars obtained by direct tensile test.*

3.3.2. Modified tensile test

The samples used in modified tensile tests are represented in figure 4 (b). Through the 14 mm diameter hole, a 12 mm diameter metallic bar is introduced and fixed by their threaded ends at the steel pipe caps. The bar stabilizes crack by providing extra stiffness. It allows to minimize or eliminate the strain energy release from the testing system. The brass bars were selected due to their elastic modulus relatively close to that of concrete and their high yield stress. During testing loading, the bar exhibits a linear elastic behaviour.

Tensile load is applied directly to the bar ends and pip caps, which transmit the load to the mortar specimen. A perfect coaxiality of the bar, sample and loading axis is necessary to obtain accurate results. Two INSTRON extensometers were mounted on the opposite sides of the sample for strain measurement as well as test control. Two strain gauges were also fixed on the opposite faces in the middle of the brass bar for strain measurement.

During the test, we recorded (figure 5 (a) and (b)):

- The total load F_{tot}.
- The longitudinal strain of the mortar ε_M recorded by the extensometers.

- The longitudinal strain of the bar ε_B recorded by the strain gauges.

Global equilibrium equation of the central section of the composite specimen (mortar sample and brass bar) is written in the following form:

$$F_{tot} = F_B + F_M = \sigma_B S_B + \sigma_M S_M$$

Where F_B and F_M are the loads applied to the brass bar and the mortar respectively. σ_B and σ_M are the tensile stresses. S_B and S_M are the sections.

During the test, the bar has a linear elastic behaviour and thus:

$$\sigma_B = E_B \varepsilon_B$$

We deduced that:

$$\sigma_M = (F_{tot} - E_B \varepsilon_B S_B)/S_M$$

where E_B is the Young's modulus of the bar obtained by direct tensile test.

The composite specimen (mortar sample and brass bar) equipped with the extensometers were mounted onto the test machine. We used an INSTRON 4505 type machine equipped with a 100 kN load cell and a PID servo control with four control channels: crosshead control, load control and two channels for strain control. The specimen was firstly loaded under crosshead control. For an increment of tensile load, the slopes of the strain-time curves of the two extensometers would exhibit some differences. The test control mode was then automatically switched to extensometer control (strain control) by choosing the one which shown the largest slope change of the strain at the time. The displacement rate was set to:5.10^{-4} mm.s^{-1}. This so-called adaptive control method was achieved by writing a Lab View© program.

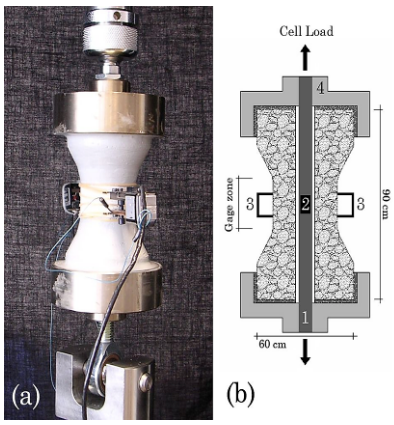

Figure 4. (a)*Direct tensile test setup. (b) Modified tensile test setup: 1 metallic brass, 2 strain gauge, 3 extensometers, 4 steel pip caps.*

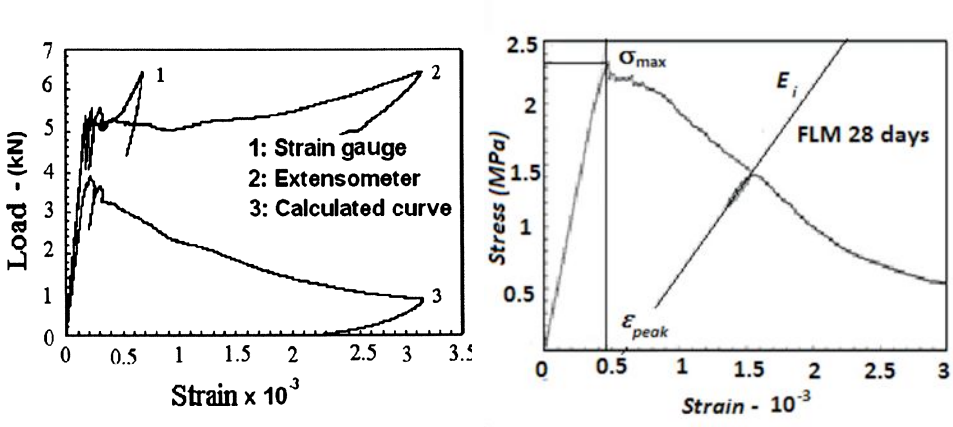

Figure 5. *(a) Typical responses recorded from strain gauge and extensometer (b) Typical stress-strain curve obtained by modified tensile test.*

3.4. *Compression tests*

The compression tests were achieved on an MTS hydraulic press (fig.6). During the tests, we measured and recorded the applied load by a 100 KN load cell, the longitudinal strain (ε_L) by an MTS extensometer, and the transversal strain (ε_T) by a setup especially designed for these tests. The transversal strain determination is based on the measure of the displacements (U1 and U2) of two opposite sample faces. This measure is achieved by two proximity sensors (sensors 1 and 2) running on eddy currents. Two aluminum targets are then needed to make the sensors working. The sensors are mounted to a support smoothly fixed on the sample. Tests on the repair mortars were achieved under longitudinal strain control at various ages between 7 and 210 days. An automatic routine of data capture and processing allows us to determine the initial Young's modulus E_0, its value at the ith unloading E_i, the maximum stress σ_{max}, the longitudinal and transversal strains $(\varepsilon_L^{peak}, \varepsilon_T^{peak})$ associated with σ_{max}. A typical stress-strain curve are plotted in figure 6.

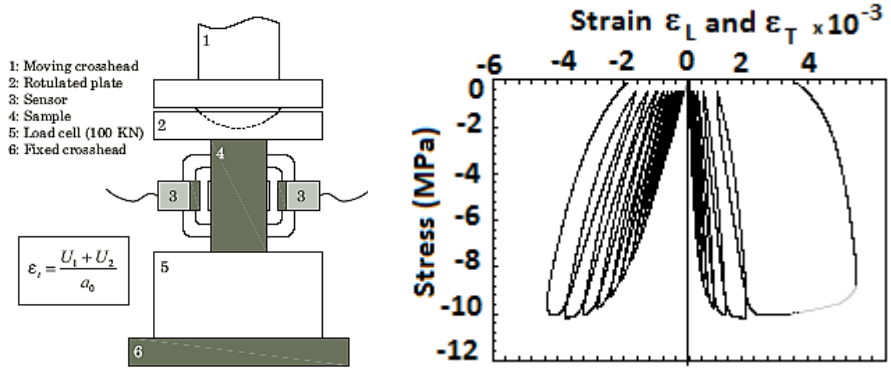

Figure 6. *Experimental setup and typical stress strain compression diagram.*

4 Results and discussions

4.1. *Mechanical behaviour of repair mortars*

Figure 7 shows the free shrinkage strains curves of the mortars stored at 23 °C and 50% RH. The repair mortars (FLM and FOM) exhibit greater shrinkage

compared with the ordinary mortar (OM). The shrinkage strains of the mortars increases greatly during the first two weeks and hardly evolves beyond four weeks. Similar results were found by Emberson *et al.* for SBR and vinyl acetate polymer modified cementitious material. From the results of shrinkage test, the risk of shrinkage cracking in these repair mortars is great without the presence of fibers (figure 7).

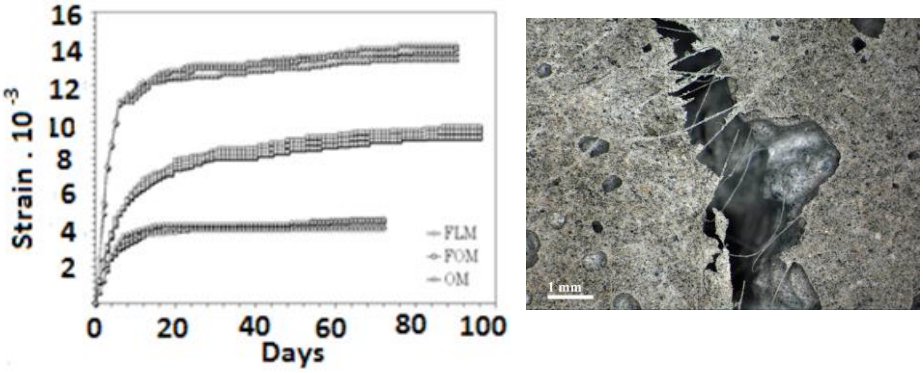

Figure 7. *Free shrinkage strain vs. the age of studied mortars and some fibers bridging cracks.*

Figure 8 and figure 9 show the envelope of load-strain curves (a) and the peak load *versus* the age in logarithmic scale of the repair mortars (b), obtained by three-point bending tests. FLM maximum load increases with time, however the mortar becomes more brittle; at 210 days mortar age, FLM samples fail brutally and it was difficult to obtain complete post-peak response by three-point bending test. The embrittlement of the FLM with time is confirmed. FOM flexural strength increases until 28 days and decreases beyond this age. The reasons accounting for the evolution of the flexural strength are not obvious. The porosity can play a major role, since the volume fraction of pores is not similar throughout the materials. We know that cement hydration strengths the cement-based materials by filling the capillary pores with hydrates, especially during the first month after their making (Folliot *et al.* 1982). The influence of a possible difference in cement hydration is not easy to handle. The cement hydration in the materials may be responsible for the bending strength evolution. Nevertheless, this is true for the FLM but not for the FOM. Cement hydration is not the only cause of the bending strength evolution presented in figure 8. The last reason we consider is the percolation of the thickening agent over the FLM samples. A film rich in thickening agent is formed on the FLM sample faces. SEM observations achieved on the FLM sample faces

revealed this film although EDS elementary analysis did not identify its precise nature. This film may limit the FLM sample from drying out and, therefore, from surface micro-cracking. On the contrary, micro-cracks on the skin of the FOM sample, due to sample drying out, would be responsible for the damage initiation (Pascal *et al.* 2004, Li *et al*. 2001).

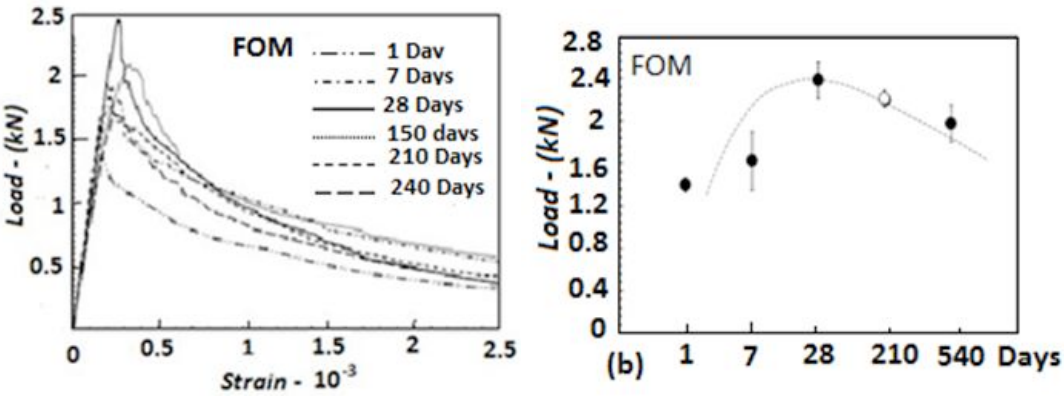

Figure 8. *Load-strain curves (a) and evolution of flexural load (FOM) (b).*

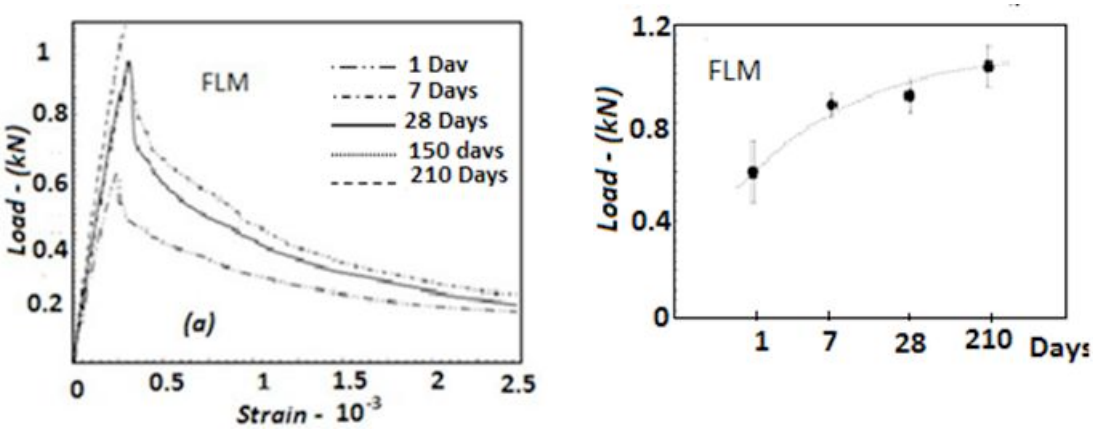

Figure 9. *Load-strain curves (a) and evolution of flexural load (FLM) (b).*

Figure 10 shows stress-strain curves of the mortars obtained at various ages by modified tensile tests. The highest tensile strength was accorded to the mortar

containing silica fume (FOM). In addition, silica fume has increased the tensile strain capacity of the FOM compared with an ordinary mortar having similar Young's modulus. The role of silica fume to increase the tensile strength is known (Jolio *et al.*2004, Emmons 1994). Although FOM tensile strength is higher than that of the FLM, however its strain at peak is lower. The highest tensile strain capacity of the FLM may be justified by its microstructure and/or the percolation of thickening agent in the matrix. Tensile tests have also allowed us to study the evolution of materials (figure 11 and figure 12). Both Young's moduli and tensile strengths of the materials increase with time. FLM evolve very slowly between 7 and 28 days, which is due to the slow carbonation and hydration processes of the mortar, significant increase of Young's modulus is observed at 150 days age.

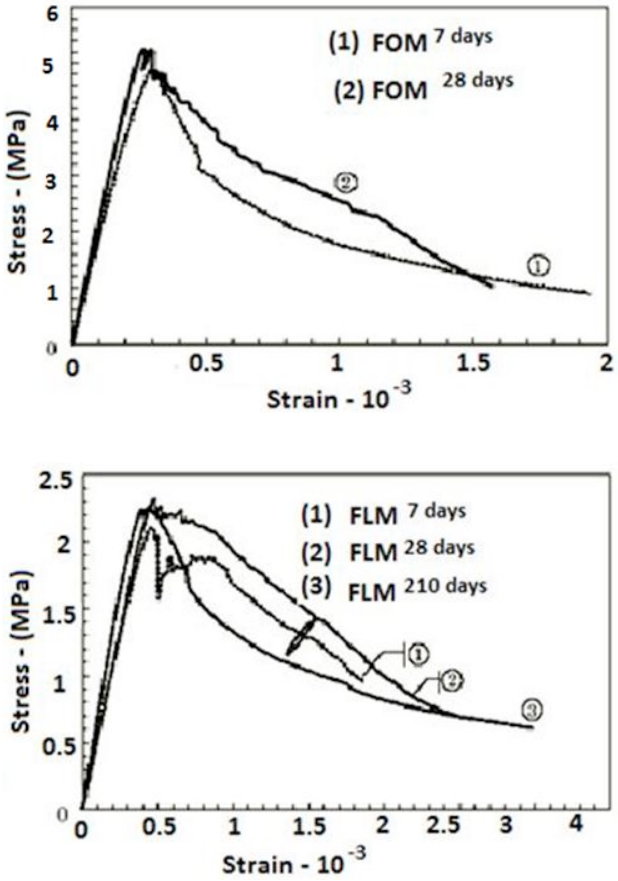

Figure 10. *Stress-strain tensile curves for FOM and FLM.*

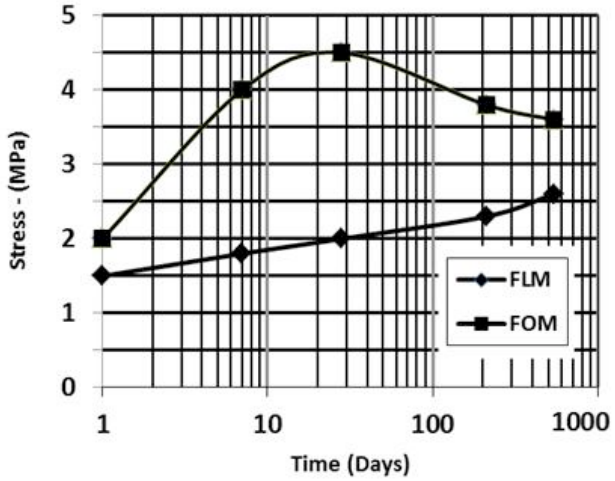

Figure 11. *Evolution of strength for FLM and FOM repair mortars.*

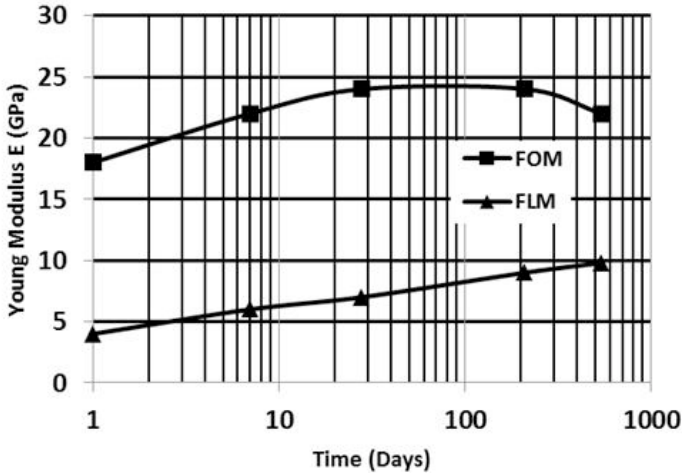

Figure 12. *Evolution of Young's modulus for FLM and FOM repair mortars.*

If the cement hydration were responsible for the bending strength evolution, this would also have a strong influence on the evolution of the compressive strength. But this is not the case of the FOM. As shown in figure 13, FOM compressive strength increases between 1 and 28 days and hardly evolves between the age of 28 and 210 days, however the bending strength decreases strongly between these two dates.

Therefore, we assume that cement hydration is not the only cause of the bending strength evolution presented in figure 8. The last reason we consider is the percolation of the thickening agent over the FLM samples. A film rich in thickening agent is formed on the FLM sample faces. SEM observations achieved on the FLM sample faces revealed this film although EDS elementary analysis did not identify its precise nature. This film may limit the FLM sample from drying out and, therefore, from surface micro-cracking. On the contrary, micro-cracks on the skin of the FOM sample, due to sample drying out, would be responsible for the damage initiation [Pascal. *et al*., Li *et al*.].

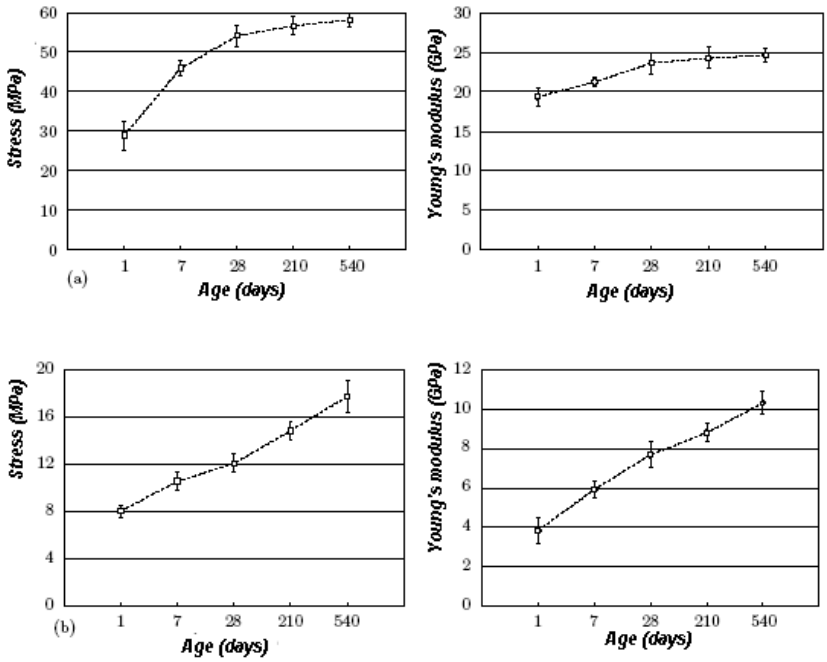

Figure 13. *Evolution of strength and Young's modulus of the repair mortars (a): FOM, (b): FLM.*

4.2. *Bond characterization*

FOM has the highest bond strength in both slant-shear and flexural bonding tests (figure 14). Slant-shear samples with engraved surface produced the highest bond strengths. Grounded (smooth) surface produced the lowest bond strengths (Franck 1986). Slant-shear test results show also that wet or saturated substrates with dry surfaces gave the highest bond strengths compared with the other moisture conditions.Emmons (Emmons *et al.* 1994) mentions that the moisture level of the substrate may be critical in achieving bond. He states that an excessively dry substrate may absorb too much water from the repair material while excessive moisture in the substrate may clog the pores and prevent absorption of the repair material. Therefore, a saturated substrate with a dry surface is considered to be the best solution. Chorinsky (Chorinsky 1996) and Mallat *et al.* (Mallat *et al*. 2006, Mallat *et al*. 2011) concluded that too dry or too wet surface of concrete substrate always results in weak bond strength of the interface. All FOM-to-substrate samples, except for those with broken surface substrate, underwent a monolithic behaviour (figure 15), contrary to FOM-to-broken surface substrate samples which especially debonding at high level of load occurred. Debonding also occurred for all FLM-to-substrate samples.

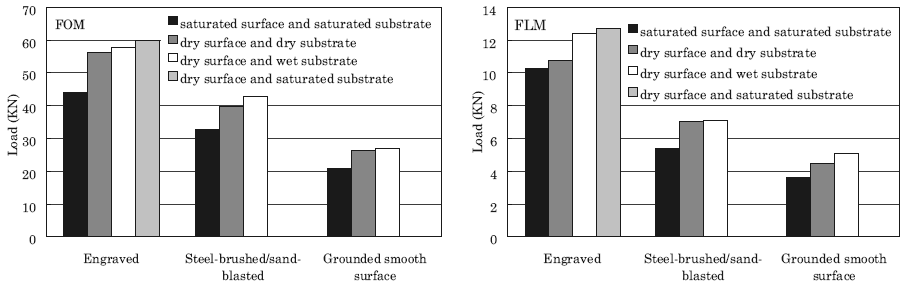

Figure 14. *Influence of moisture condition and surface roughness on shear bonding strength.*

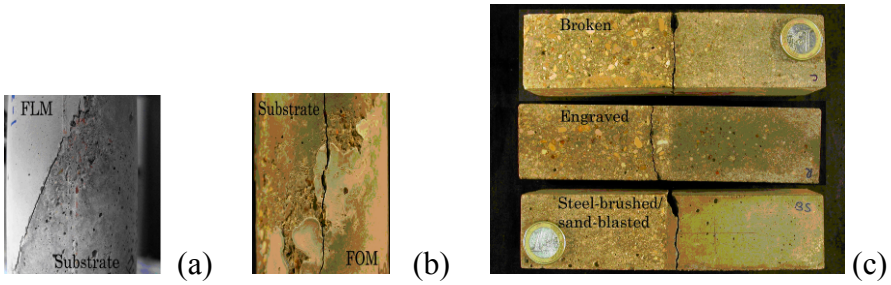

Figure 15. *Failure mode of repair mortars-to-substrate samples by slant shear test (a) and (b) and flexural test (c).*

For the flexural bonding tests, all substrates were saturated with dry surfaces. FOM to engraved substrate surface produced the highest bond strength. However, the same surface type produced the lowest bond strength in the case of FLM, which indicates that the bonding behaviour of different materials may change even if they are applied on the same type of surface. In addition, bond strength values of FOM to substrate were between the flexural strength values of the two basic mortars (FOM and substrate (figure 14 (c)). This is not true for the FLM where the bond strength values were lower than the flexural strength values of the basic mortars. It shows the repair mortars-to-substrate interfacial zone. Figure 16 highlights an obvious separations between substrate and FLM accompanied by a high concentration of micro-cracks in the matrix. The micro-cracks are orthogonal to the sand grains and they are probably induced by the great shrinkage of the paste. SEM observations also show many large interfacial transition zones resulting from weak bond between paste and aggregates. Shrinkage cracking exists at all repair interfaces due to differential shrinkage between the hardened substrate and the freshly laid plastic overlay. Under an applied load, these flaws cause stress concentrations and render the interface weak. This is the case of the FLM: significantly pronounced shrinkage cracking may be expected to occur at the repair interface. The low bond strength between substrate and FLM may also be related to the presence of the thickening agent in the mortar. In this case, a film rich in thickening agent may be formed at the interface and the bond of new-to-old mortar depends mainly on glutinous nature of the thickening agent (molecular force). Finally, the high content of large portlandite crystals between the film and the matrix weakens this zone. The failure will probably occur through this zone. The interfacial zone of FOM-to-substrate is more dense and uniform, and few cracks and interfacial transition zones were observed (Fig.15): chemically, the silica fume reacts pozzolanically with calcium hydroxide produced by the hydration of cement to produce a greater solid volume of calcium silicate hydrate gel, leading to an additional reduction in capillary porosity and

decreases the calcium hydroxide (weak large crystal) content in the matrix Chorinsky 1996, Li and Xiong 2001, Jolio and al. 2004). Physically, the numerous silica fume particles in the FOM fill the weak spaces of interfacial and interfacial transition zones making them denser and more homogeneous (Climaco *et al.* 1989, Knab *et al.* 1989). The good bond between FOM paste and sand grains prevents the propagation of cracks through the transition zone.

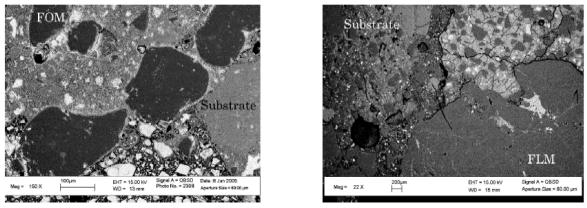

Figure 16. *Back scattered electron SEM micrograph of interfacial zones of repair mortars 90 days old-to-substrate 80 years old.*

5. Conclusion

The test results described in this paper indicate that synthetic fibers and thickening agent would not modify the nature of the cement hydration products. The slow carbonation of portlandite and the thickening agent slow down the evolution of the Fiber-reinforced Lime-based mortar (FLM) mechanical properties. The flexural strength of Fiber-reinforced Ordinary Mortar (FOM) increases until 28 days and decreases after this age. The FLM flexural strength remains increasing with time. The increase of the FLM flexural strength and the presence of thickening agent in the mortar match. Since the influence of porosity is difficult to verify and a difference in cement hydration cannot explain this evolution, it is suggested that the percolation of the thickening agent over the sample increases its flexural strength. The thickening agent may prevent the material from skin micro-cracking which could be the cause of the early damage initiation into the mortar. On the contrary, micro-cracks on the skin of the FOM sample, due to sample drying out, would be responsible for the damage initiation. Tensile tests results show that fibers and silica fume enhance the tensile strength and strain capacity of mortars.

The bonding test results show that both surface roughness and moisture conditions of substrate has a significant influence on the bond strength even if the

FLM is less sensitive to surface type. Microcracking due to differential shrinkage between substrate and FLM weakens the bond and induces a lower failure load. However, silica fume in the FOM increases the mechanical properties of the repair mortar-to-substrate interfacial zone and interfacial transition zones, thus leading to a better bond.

6. References

Chorinsky E. G. F. "Repair of concrete floors with polymer modified cement mortars". *RILEM Symposium Adhesion between polymers and concrete*. Chapman and Hall, London, 1986, p. 230-234.

Climaco J.C., Regan P.E. "Evaluating of bond strength between old and new concrete". In Forde M. Editor. International Conference on structural faults and repair. Vol.1 London: Engineering Technique Press, 1986, p. 115-122.

Emberson N. K.,, Mays G. C. "Significance of property mismatch in the patch repair of structural concrete". Part I; *Magazine of Concrete Research,* 1996, vol. 174 no. 48, p. 45-57.

Emmons P. H. "Bonding repair materials to existing concrete". *Concrete repair and maintenance*. M. A. R.S. Means Company, 1994, p.154-163.

Folliot A., Buil L. La structuration progressive de la Pierre de ciment, in: *Le béton hydraulique : connaissance et pratique*. Presse de l'ENPC. Paris 1982.

Franck L. "The dimensioning of adhesive-bonded joint in concrete building components". *Intenational RILEM symposium in adhesion between polymers and concrete*. London: Chapman and Hall, 1986, p. 447-461.

Julio E. N. B. S., Branco F.A.B., Silva V.D., "Concrete-to-concrete bond strength, influence of the roughness of the substrate surface". *Construction and Building Materials* 2004, vol. 9 no. 18, p. 675-681.

Knab L., Spring C. B. "Evaluation of test methods for measuring the bond strength of Portland cement based repair material to concrete". *Cem. Concr. Aggregate*, 1989, vol.11, p. 3-14.

Li G., Xie H., Xiong G. "Transition zone studies of new-to-old concrete with different binders". *Cement and Concrete Composites*, 2001, vol. 23, p. 381-387.

Mallat A., Alliche A. "Physico-chemical and mechanical behaviour of fiber reinforced repair mortars". *Third International Conference on FRP composites in civil engineering (CICE 2006)*, Miami, USA, Dec. 2006.

Mallat A., Alliche A., "A modified tensile test to study the behaviour of cementitious materials". *Strains,* 2011, vol. 6 no. 6, p. 499–504.

Mangat P., Limbachiya M. "Repair material properties for effective structural application". *Cement and concrete Research*, 1997, vol. 27, p. 601-617.

Pascal S., Alliche A., Pilvin P. “Mechanical behaviour of polymer modified mortars”. *Materials Science and Engineering* A. 2004, vol.380, p. 1-8.

Ramtani S. “ Contribution à la modélisation du comportement multiaxial du béton endommagé avec description du caractère unilatéral”. PHD Thesis ; Université Paris 6 - France – 1990;

Tabor L. J. “The evaluation of resin systems for concrete repair”. *Mag. Concr. Res.* 1978, vol. 30, p.221-225

Wall J.S, Shrive N.G. “Factors affecting bond between new and old concrete”. *ACI Mater.Journal*, 1998, vol. 2 no. 85, p. 117-125.